Asymmetric p38 Activation in Zebrafish: Its Possible Role in Symmetric and Synchronous Cleavage

Ritsuko Fujii, Susumu Yamashita, Masahiko Hibi, and Toshio Hirano

Division of Molecular Oncology, Biomedical Research Center (C-7), Osaka University Graduate School of Medicine, Suita, Osaka 565-0871 Japan

Abstract. Cleavage is one of the initial steps of embryogenesis, and is characterized by a series of symmetric and synchronous cell divisions. We showed that p38 MAP kinase (p38) is asymmetrically activated on one side of the blastodisc during the early cleavage period in zebrafish (*Danio rerio*) embryos. When a dominant negative (DN) form of p38 was uniformly expressed, blastomere cleavage was impaired on one side of the blastodisc, resulting in the formation of blastomeres with a large mass of cytoplasm and an enlarged nucleus on the affected side. The area affected by the DN-p38 expression did not correlate with the initial cleavage plane, but coincided with the side where *dharma/bozozok*, a dorsal-specific zygotic gene, was expressed (Yamanaka et al., 1998). Furthermore, UV irradiation and removal of the vegetal yolk mass before the first cleavage, both of which inhibit the initiation of the dorsalizing signals, abolished the asymmetric p38 activation. Our findings suggest that asymmetric p38 activation is required for symmetric and synchronous cleavage, and may be regulated by the same machinery that controls the initiation of dorsalizing signals.

Key words: zebrafish • p38 • asymmetry • cleavage • microtubules

Introduction

In all animal species, cleavage initiates the production of a multicellular organism from a single fertilized egg. In some invertebrates, cleavage asymmetrically segregates maternally deposited cell fate determinants into the daughter cells, probably by regulating the orientation of the mitotic spindle and the timing of its formation. In contrast, cleavage in vertebrate embryos is characterized as a series of symmetric and synchronous cell divisions without a net increase in cell mass, and is controlled by unknown mechanisms (Kane, 1999).

In zebrafish (*Danio rerio*) embryos, cleavage progresses symmetrically and synchronously. During the cleavage period, the cell cycle consists of mitosis and a short interphase, so that the cleavage cycle proceeds synchronously and rapidly with a periodicity of ~15 min during the first 12 divisions (Kane, 1999). Although cleavage is well understood at descriptive level (Kane, 1999), it is not understood how the cleavages are regulated to symmetrically and synchronously proceed.

Address correspondence to Toshio Hirano, Division of Molecular Oncology (C-7), Biomedical Research Center, Osaka University Graduate School of Medicine, 2-2 Yamada-oka, Suita, Osaka 565-0871 Japan. Tel.: 81-6-6879-3880. Fax: 81-6-6879-3889. E-mail: hirano@molonc.med.osaka-u.ac.jp

Soon after the series of synchronous cleavages, zebrafish embryos display asymmetry with respect to their dorso-ventral axis. Several zygotic genes, including *dharma/bozozok*, are expressed specifically in the dorsal blastomeres during the mid-blastula period (Yamanaka et al., 1998; Kodjabachian et al., 1999). Several lines of evidence suggest that dorsalizing signals could be initiated during the early cleavage period. Depletion of the vegetal yolk mass or disruption of the yolk cortical microtubules during the early cleavage period abolishes the initiation of dorsalizing signals, consequently, dorsal gene expression is extinguished and the embryo is ventralized (Jesuthasan and Stahle, 1997). These studies led to the hypothesis that the dorsal determinants are initially localized at the vegetal pole, and then are transported to the dorsal blastodisc through the cortical microtubule array as early as the 16–32-cell stages, at which point they activate the dorsalizing signals (Driever, 1995; Jesuthasan and Stahle, 1997). Consistent with this hypothesis, small organelles and Dishevelled, a potential activator for the dorsalizing signals, are transported to the dorsal side of the embryo through a microtubule array in *Xenopus* (Larabell et al., 1997; Moon and Kimelman, 1998; Miller et al., 1999). However, it is completely unknown whether the mechanisms that control the dorso-ventral axis determination are involved in the establishment of asymmetry in other systems.

Mitogen-activated protein kinase (MAPK)[1] signal transduction cascades are well conserved from yeast to mammals (Garrington and Johnson, 1999). To date, three distinct MAP kinase pathways have been defined in eukaryotes: the extracellular signal–regulated kinase, C-Jun N-terminal kinase (JNK; Davis, 1999), and p38 (Han et al., 1994) pathways. Although there is a growing understanding of the roles played by the p38 signaling pathway in mammalian cell lines, its role in development has been relatively unexplored. One recent study has shown that *licorne* (*lic*), a *Drosophila* MAPK kinase (MAPKK) belonging to the p38 MAPKK family, plays an essential role in anterior-posterior and dorsal-ventral patterning during oogenesis by regulating the localization of cell fate determinants (Suzanne et al., 1999). This evidence raised the possibility that the p38 pathway, which is well conserved across species, may also play an intrinsic role in establishing the initial asymmetry in other organisms.

Here, we show that p38 is activated asymmetrically in zebrafish during the early cleavage period and that suppression of p38 activation inhibited cytokinesis on one side of the blastodisc. We demonstrate that the side where the cleavage is disrupted coincides with the future dorsal side of the embryo. Disruption of the microtubule array and removal of the vegetal yolk hemisphere not only abolished the dorsal gene expression, but also abolished the asymmetric activation of p38. Our results indicate a novel role for the p38 cascade in controls of blastomere cleavage.

Materials and Methods

Molecular Cloning of Zebrafish MAP Kinases

cDNA fragments for zebrafish MKK3 (MAP kinase kinase 3), p38a, p38b, and JNK were isolated by screening a λgt10 18–h postfertilization (hpf) embryo cDNA library (gift from H. Okamoto, RIKEN, Wako, JAPAN) by hybridization with human MKK3 (PCR product, a gift from Dr. Sugiyama, Boehringer Ingelheim Co.), carp p38, and JNK cDNAs (gift from Drs. Hashimoto and Toyohara, Kyoto University, Kyoto, Japan). Entire coding fragments of the cDNAs were obtained by 5′ RACE from an adult fish cDNA library using a Marathon cDNA amplification kit (CLONTECH Laboratories, Inc.) according to the manufacturer's protocol. Zebrafish p38a, p38b, JNK, and MKK3 cDNA sequences have been deposited in the GenBank database under accession numbers, AB030897, AB030898, AB030900, and AB030899, respectively.

Constructs

Point mutations were generated by a two-step PCR protocol (Ho et al., 1989). The dominant negative form of zebrafish p38a (DN-p38a) and p38b (DN-p38b) was prepared by replacing the threonine and tyrosine residues in the conserved dual phosphorylation motif (TGY) (Lee et al., 1994) with alanine and phenylalanine (AGF), respectively. The dominant negative form of zebrafish MKK3 (DN-MKK3) was prepared by replacing lysine in the putative ATP-binding domain with alanine (Mansour et al., 1994; Raingeaud et al., 1995). The constitutively active form of zebrafish MKK3 (CA-MKK3) was constructed by replacing the serine and threonine residues in the conserved dual phosphorylation site (SVAKT) with negatively charged glutamates (EVAKE) (Mansour et al., 1994). All of these constructs, with or without mutations (WT-p38, WT-p38b, and WT-MKK3), were subcloned into the pCS2+ expression vector (Rupp et al., 1994) with a sequence tag (Myc-tag for p38a, p38b, and JNK). A fragment encoding three tandem repeats of hemagglutinin epitopes was excised from pSRα-HA-JNK1 (Derijard et al., 1995) and fused to the MKK3 cDNA followed by subcloning into the pCS2+ expression vector. Capped mRNAs were synthesized in vitro using the linearized plasmid DNA of the constructs as a template. Microinjection was performed as previously described (Westerfield, 1995).

Western Blot Analysis

293T cells were seeded on 6-cm cell culture dishes and transfected at 70% confluency with plasmid DNAs containing the p38, MKK3, JNK, or human constitutively active form of zebrafish MKK4 (CA-MKK4; a gift from Dr. Sugiyama, Boehringer Ingelheim Co.) constructs (5 μg each) by a standard calcium phosphate precipitation method. After 18 h, the cells were lysed on ice for 15 min in RIPA buffer (PBS containing 1% NP-40, 0.5% sodium deoxycholate, and 0.1% SDS, pH 7.4, 4 mM PMSF, 10 μg/ml aprotinin, 1 mM sodium vanadate, 30 mM pyrophosphate, and 50 mM NaF). The lysates were cleared by centrifugation for 5 min at 10,000 rpm at 4°C. After immunoprecipitation with an anti–Myc-tag antibody (9E10 mouse mAb; Santa Cruz Biotechnology, Inc.), Western blots of the immunoprecipitated Myc-p38 proteins were probed with either 9E10 antibody (1:2,000 dilution) or anti–dual-phosphorylated p38 rabbit polyclonal antibody (anti–dp-p38 antibody or anti–ACTIVE p38™; Promega), which specifically recognizes the active state of p38, which is dually phosphorylated at threonine and tyrosine residues within the conserved motif (Raingeaud et al., 1996). Chemiluminescent detection was performed using the RENAISSANCE™ Western blot reagent (DuPont-NEN).

For in vivo activation of endogenous p38 proteins, RNAs for WT- or DN-p38a and DN-MKK3 were injected to the one-cell stage embryos. The injected or noninjected embryos were collected at 2.5 hpf (256-cell stage), dechorionated, and lysed in SDS sample buffer (63 mM Tris-HCl, pH 6.8, 10% glycerol, 100 mM DTT, and 3.5% SDS). The lysates were boiled for 5 min and cleared by centrifugation. The protein was immunoblotted by anti-p38 rabbit polyclonal antibody (C-20; Santa Cruz Biotechnology, Inc.) or anti–ACTIVE p38™ rabbit polyclonal antibody (Promega).

Luciferase Reporter Assay

The luciferase assay was performed using PathDetect™ in vivo signal transduction pathway trans-reporting systems (Stratagene). 293T cells were seeded on 6-cm cell culture dishes and transfected at 70% confluency using a standard calcium phosphate precipitation method. To control the luciferase expression, we transfected the cells with expression vectors containing an activation domain of human ATF2 fused to the DNA-binding domain of yeast GAL4 (0.2 μg) named pFA-ATF2 and a luciferase reporter containing a synthetic promoter with five tandem repeats of the yeast GAL4-binding sites (5×GAL4-luciferase; 2 μg). These constructs were cotransfected with one of the p38 or MKK3 constructs, or with the pCS2+ vector alone as the vector control (5 μg) and an expression vector for β-galactosidase as an internal control (2 μg). Luciferase activity in each transfectant was determined using the PicaGene™ luciferase assay system (Toyo Ink, Tokyo). β-Galactosidase, which was cloned into the pCS2+ expression vector, was used for normalizing transfection efficiency.

Reverse Transcriptase (RT)–PCR

Embryos were collected at the indicated stages and total RNA was prepared using the TRIzol™ reagent (Gibco BRL). 1 μg of total RNA was used to prepare cDNAs by Superscript™ RT (GIBCO BRL) according to the manufacturer's protocol. One fiftieth of the cDNA was used for PCR. After 25 cycles of PCR using specific primer pairs for p38a, p38b, MKK3, and Max for an internal control, one tenth of the total reaction was electrophoresed on 1.5% agarose gel. To ensure the fidelity of the primer pairs, pBluescript™ (Stratagene) clones of cDNA s for p38a, p38b, and MKK3 (25 ng) were also subjected to the PCR.

Confocal Immunofluorescence Microscopy

Embryos were dechorionated and fixed in 4% paraformaldehyde over-

[1]*Abbreviations used in this paper:* anti–dp-p38 antibody or anti–ACTIVE p38™, anti–dual-phosphorylated p38 rabbit polyclonal antibody; BrdU, 5-bromo-2′-deoxyuridine; CA-MKK3, constitutively active construct of zebrafish MKK3; CA-MKK4, constitutively active construct of MKK4; DDs, dorsal determinants; DN-MKK3, dominant negative construct of zebrafish MKK3; DN-p38a, dominant negative construct of zebrafish p38a; Dvl, Dishevelled; hpf, hours postfertilization; JNK, C-Jun N-terminal kinase; *lic*, *licorne*; MAPK, mitogen-activated protein kinase; MAPKK or MKK, MAPK kinase; mpf, minutes postfertilization; RT, reverse transcriptase; YSL, yolk syncytial layer.

night at 4°C. After several washes in PBS, pH 7.4, the embryos were permeabilized in methanol overnight at –20°C. The fixed embryos were bisected from the yolk hemisphere and rehydrated with PBS. The bisected, fixed embryos with their blastodiscs were incubated in 1% blocking solution (blocking reagent; Boehringer Mannheim) containing 20% normal goat serum, 1% DMSO, and 0.1% Triton X-100, for 1 h at room temperature, and further incubated with anti-p38 rabbit polyclonal antibody (C-20; Santa Cruz Biotechnology, Inc.) or anti–ACTIVE p38™ (Promega). Anti-p38 antibody was used at a 1:100 dilution and anti–ACTIVE p38™ antibody was used at a 1:50 dilution. The secondary antibody was biotinylated goat anti–rabbit (Vector Laboratories) used at a 1:200 dilution. Protein localization was determined after incubation in UltraAvidin™-rhodamine (1:50 dilution; Leinco Technologies Inc.). Images were obtained at a depth of 70–100 μm from the animal pole surface by an inverted microscope (Zeiss Axiovert 135M) connected to a confocal laser scanning microscope (model LSM410; Carl Zeiss, Inc.). To detect Myc-tagged proteins, an anti–Myc-tag antibody (9E10 mouse mAb, Santa Cruz Biotechnology, Inc.) was used as the primary antibody.

BrdU and Phalloidin Stainings

Embryos were injected first with DN-p38 (125 pg) at 15 mpf, and then at 20 mpf with 500 pl of 5 mM 5-bromo-2′-deoxyuridine (BrdU). After fixation in 4% paraformaldehyde, embryos were washed in PBS, pH 7.4, and treated with 4 M HCl for 15 min at room temperature. After washing, embryos were blocked and stained with fluorescein-conjugated anti–mouse BrdU antibody using the in situ cell proliferation kit-FLUOS® (Roche) according to manufacturer's protocol. For phalloidin stainings, the stained embryos were washed in phosphate buffer, pH 7.2, containing 0.1% DMSO and soaked in 1 μM rhodamine-phalloidin (Molecular Probes).

Cell Tracing

DN-p38a RNA (125 pg) was injected into the yolk cells 10–15 min postfertilization (mpf), followed by the injection into one blastomere at the two-cell stage of a 1:1 mixture of 0.5% dextran tetramethylrhodamine (2,000 kD; Molecular Probes) and 0.5% lysine-fixable biotin-dextran (2,000 kD; Molecular Probes; Abdelilah et al., 1994; Helde et al., 1994). In another experiment, DN-p38 RNA was injected together with the tracer dye mixture into one blastomere of the embryo at the two-cell stage. Within 20 min, the labeled embryos were screened using a Zeiss Axioplan microscope with epifluorescence optics to discard any embryos with leaks, variable intensity of the injected dye, or abnormal morphology. After 3 h, embryos were fixed in 4% paraformaldehyde, embedded in Technovit 8100 (Heraeus Kulzer), and sectioned. The 8-μm sections were viewed with a fluorescence microscope (Zeiss Axioplan2) and photographed with a CCD camera (model HC-2500 3p; Fuji Photo Film Co.). Superimposition of the images and figures was constructed using Adobe Photoshop® version 5.

Whole-mount In Situ Hybridization

Normal embryos were fixed in 4% paraformaldehyde. DN-p38a–injected embryos were fixed at the equivalent developmental time for the high stage, judging from their shapes and the size of the blastomeres. Whole-mount in situ hybridization for *dharma* was performed as previously described (Yamanaka et al., 1998). The processed embryos were refixed in 4% paraformaldehyde, washed in PBS, and then either mounted in 100% glycerol for photography or dehydrated and embedded in Technovit 8100 for sectioning.

UV Irradiation and Yolk Depletion

Embryos were irradiated with the chorion intact with 312 nm of UV light for 10 min using Fluor-link (ATTO), and fixed at the two- or four-cell stage. Unfixed irradiated embryos were allowed to develop until 24 hpf to assess their viability and ventralized phenotypes. Yolk depletion was performed essentially as previously described (Mizuno et al., 1999a).

Results

Asymmetric p38 Activation at Early Cleavage Stages

To investigate the functions of p38 signaling in zebrafish embryogenesis, we isolated cDNAs for the zebrafish orthologues of the p38 MAP kinase, p38a and p38b, and its upstream activator, MKK3 (Han et al., 1994; Raingeaud et al., 1996; Garrington and Johnson, 1999). RT-PCR (Fig. 1 A) was performed to examine the temporal expression of these gene products. During the cleavage period, p38a and MKK3 transcripts were all maternally deposited, and zygotic expression was detected throughout development. The expression level of p38b was hardly detectable during cleavage stages (Fig. 1 A, 1–3 hpf). As p38b appeared to function as a redundant form of p38a, we used the p38a clone in this study. The amino acid sequences of zebrafish p38a (361 amino acids) and p38b (348 amino acids) exhibited 86 and 64% identity with human p38, respectively (Raingeaud et al., 1995), and zebrafish MKK3 shared 77% identity with human MKK3 (Raingeaud et al., 1996). The threonine-glycine-tyrosine (TGY) motif in kinase domain VIII of p38 (Raingeaud et al., 1995), in which the threonine and tyrosine are dually phosphorylated by MKK3 or MKK6 (Raingeaud et al., 1996), was also present in zebrafish p38a and p38b, suggesting that the MKK3/MKK6-p38 signaling pathways are conserved between zebrafish and higher vertebrates.

Next, we investigated the in vivo activation of p38 using anti–dp-p38 antibody (anti–ACTIVE p38™ antibody) that recognizes the dually phosphorylated active form of p38 (pTGpY). We constructed expression vectors for dominant negative (DN) forms of p38a, p38b, and MKK3, and CA-MKK3. The DN-p38s was constructed by replacing the threonine and tyrosine in the TGY motif with alanine and phenylalanine, respectively. DN-MKK3 was constructed by replacing a lysine in the ATP-binding domain with alanine (Raingeaud et al., 1996), and CA-MKK3 was constructed by replacing the serine and threonine residues in the known phosphorylation site with glutamate (Raingeaud et al., 1996). Both the wild-type (WT) and DN-p38 proteins were expressed as Myc-tagged proteins.

We first examined whether anti–dp-p38 antibody (anti–ACTIVE p38™ antibody) also recognized activated zebrafish p38. When we transfected human 293T cells with expression vectors for WT-p38a together with CA-MKK3, immunoprecipitated zebrafish p38a was recognized by the anti–ACTIVE p38™ antibody (Fig. 1 B, lane 1). In these transfected cells, activated p38 was detected in the nuclei and activation of endogenous p38 by CA-MKK3 was not significant (data not shown). In contrast, when the expression vector for DN-p38a or DN-MKK3 was transfected together with those for CA-MKK3 and WT-p38a, the antibody did not react with zebrafish p38 (Fig. 1 B, lane 2 and 3). The anti–ACTIVE p38 antibody did not react with zebrafish JNK (WT-JNK) when it was overexpressed with its activator, human CA-MKK4 in 293T cells (Fig. 1 B, bottom panel, left). Zebrafish p38b (WT-p38b) was also activated by CA-MKK3, and suppressed by DN-p38b and DN-MKK3 in 293T cells (Fig. 1 B, lanes 7–9). These results established the specificity of the antibody for activated p38.

Both DN-MKK3 and DN-p38a were effective in inhibiting the activation of WT-p38a by UV irradiation in 293T cells (Fig. 1 B, lanes 4–6). These proteins also inhibited the activation of pFA-ATF2 (see Materials and Methods;

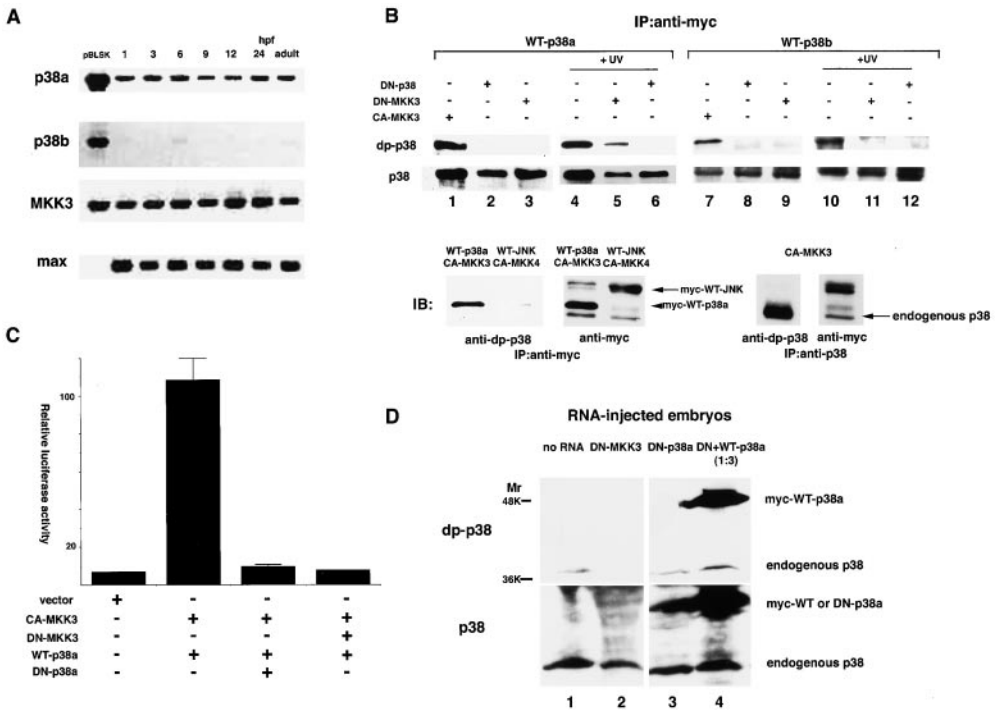

Figure 1. Functional activity of zebrafish p38 and MKK3. (A) Expression levels of zebrafish p38a, p38b, and MKK3 throughout development. RT-PCR for zebrafish p38a, p38b, and MKK3 cDNAs are shown. pBLSK, positive control for specific primer pairs for zebrafish p38a, p38b, and MKK3 cDNA clones. max, loading control. (B) Activity of zebrafish p38 and MKK3 mutants expressed in 293T cells. Western blot of cell lysates from 293T cells transfected with expression vectors for WT-p38a, DN-p38a, WT-p38b, DN-p38b, DN-MKK3, CA-MKK3, or WT-JNK and human CA-MKK4 are as indicated. Activation of WT-p38a was detected in 293T cells expressing WT-p38a and CA-MKK3 by the anti–dp-p38 antibody (anti–ACTIVE p38™ antibody; lane 1) or in the cells treated with UV light (lane 4). No activation of WT-p38a was detected in the cells overexpressing either DN-p38a (lane 2) or DN-MKK3 (lane 3). DN-p38a and DN-MKK also suppressed UV-induced activation of WT-p38a (lanes 5 and 6). Activation of WT-p38b was also detected in 293T cells expressing WT-p38b and CA-MKK3 (lane 7) or in the cells treated with UV light (lane 10), but not in the cells expressing DN-p38b or DN-MKK3 (lanes 8, 9, 11, and 12). p38 (lanes 1–12), the amount of WT-p38a and WT-p38b loaded that was detected with the anti-myc antibody. Myc-tagged WT-JNK, which was coexpressed with human CA-MKK4 in 293T cells, did not react with the anti–dp-p38 antibody (bottom panel, left). Endogenous p38 in 293T cells expressing CA-MKK3 reacted with the anti–dp-p38 antibody, but not with anti-myc antibody (bottom panel, right). (C) Activation of ATF2 in cells expressing MKK3. 293T cells were transfected with the GAL4-ATF2 (pFA-ATF2) expression vector and GAL4-dependent luciferase reporter construct together with the expression vectors for WT-p38a, DN-p38a, CA-MKK3, or DN-MKK3 constructs, or with the empty vector to control for endogenous p38 activity. Luciferase activity was measured in cell extracts and normalized against β-galactosidase activity as an internal control. The relative value of the luciferase activity was plotted. Error bars represent the SD ($n = 3$). (D) Endogenous p38 activation in zebrafish embryos. Embryos were injected with RNA (125 pg) for DN-MKK3, DN-p38a, WT-p38a as indicated. Protein extracts of the embryos at the early blastula stage were immunoblotted with anti–ACTIVE p38™ antibody. Amounts of endogenous p38, DN-p38a, or WT-p38a were detected by anti-p38 antibody (bottom).

Gupta et al., 1995), which was induced by the expression of CA-MKK3 in human 293T cells (Fig. 1 C). Moreover, injection of RNAs (125 pg) for both DN-MKK3 and DN-p38a suppressed endogenous p38 activation in the embryos (Fig. 1 D, lanes 2 and 3). Excess amount of WT-p38a (threefold molar) restored the p38 activation that was suppressed by DN-p38a (Fig. 1, lane 4). These results confirmed the dominant negative activities of both DN-MKK3 and DN-p38a on zebrafish p38. Whole-mount immunostaining of the cleavage stage embryos using the anti–ACTIVE p38™ revealed that activated p38 was expressed asymmetrically, on one side of the blastodisc at the two-cell stage, while the endogenous p38 proteins were evenly distributed (Fig. 2 A). A clear gradient of this asymmetric activation was observed towards either the first cleavage plane (Fig. 2 B) or the future second cleavage plane (Fig. 2 C), indicating that asymmetric activation was independent of the site of the first cleavage plane. The asymmetric activation gradually faded out around the 8-cell stage, which showed a uniform pattern (Fig. 2, H and I), and had clearly disappeared by the 16-cell stage, which showed a uniform (Fig. 2 K) and sometimes reduced (Fig. 2 L) activation pattern. These results suggest a role for p38 within a specific window of time during the early cleavage stage.

Suppression of p38 Activation Impairs Symmetric and Synchronous Cleavage

To elucidate the function of the asymmetric p38 activation, we injected synthetic RNAs for DN-p38a, and DN-MKK3 into zebrafish embryos. Cleavage disruption phenotypes occurred in a dose-dependent manner in the range from 50 to 500 pg of DN-p38a RNA; however, doses >500 pg were toxic. 125 pg was optimal for inducing the cleavage defect phenotype, with 82% of the embryos displaying the defect when the RNA was injected into the blastodisc of one-cell stage embryos within 15 mpf (Fig. 3 and Table I).

To confirm that the phenotypes were the result of blocking p38 activation, we also treated the fertilized embryos with SB203580, an imidazole compound proven to be a

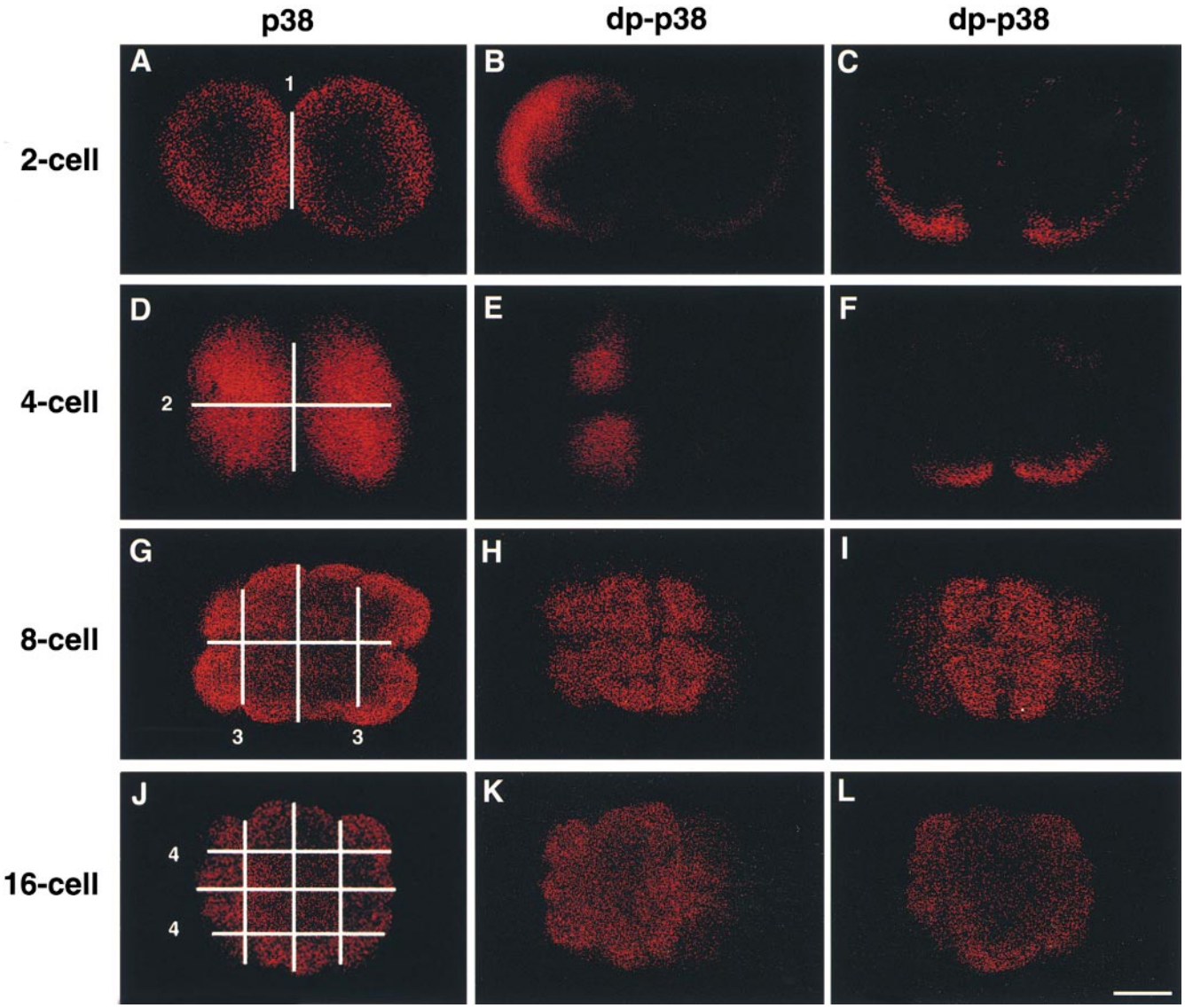

Figure 2. Asymmetric activation of zebrafish p38 during the early cleavage period. Top view of zebrafish embryos after fluorescent immunostaining with the anti-p38 antibody at the 2-cell (A), 4-cell (D), 8-cell stage (G), and the 16-cell stage (J), or with anti–dp-p38 antibody (anti–ACTIVE p38™ antibody) at the 2-cell (B and C), 4-cell (E and F), 8-cell (H and I), and the 16-cell stage (K and L). The distribution of p38 or activated p38 (red) was determined using a confocal microscope. Images were taken at a depth of 100 μm from the animal pole surface. Bar, 100 μm.

specific inhibitor for p38 kinase activity (Lee et al., 1994; Enslen et al., 1998). When embryos were treated before 15 mpf with 100 μM SB203580, they exhibited similar impaired cleavage phenotypes to those observed in the DN-injected embryos. In contrast, incubation in DMSO (0.25%) alone did not cause abnormal cleavage (Table II). In DN-p38a RNA-injected embryos, the blastomeres on one side underwent cell divisions, whereas those on the other side remained undivided (Fig. 3, F–I and J–L). At the sphere stage (~4 hpf), half of the blastoderms in these embryos was filled with abnormally large cells with an enlarged nucleus. The other half was composed of cells that had divided normally and were of normal size (Fig. 3, compare O and P to M and N, respectively). In contrast, uninjected control embryos underwent synchronous cleavage and successively generated 4, 8, and 16 equal-sized blastomeres (Fig. 3, A–D and Q).

To ensure that the impaired cleavage phenotype was not caused by biased distribution of the injected RNA, DN-p38a–injected embryos displaying the impaired cleavage phenotype were immunostained with the anti–Myc-tag antibody, which showed that the Myc-tagged DN-p38a protein was distributed evenly over the blastodisc (Fig. 3 F′, displaying the same phenotype as in F). Coinjection of WT-p38a with DN-p38a normalized the DN-induced phenotypes in a dose-dependent manner (Table I), with a threefold molar excess of WT-p38a RNA rescuing the cleavage disruption caused by the expression of DN-p38a and also endogenous dual phosphorylation of p38 (Fig. 1 D, lane 4). In contrast, JNK was not able to rescue the

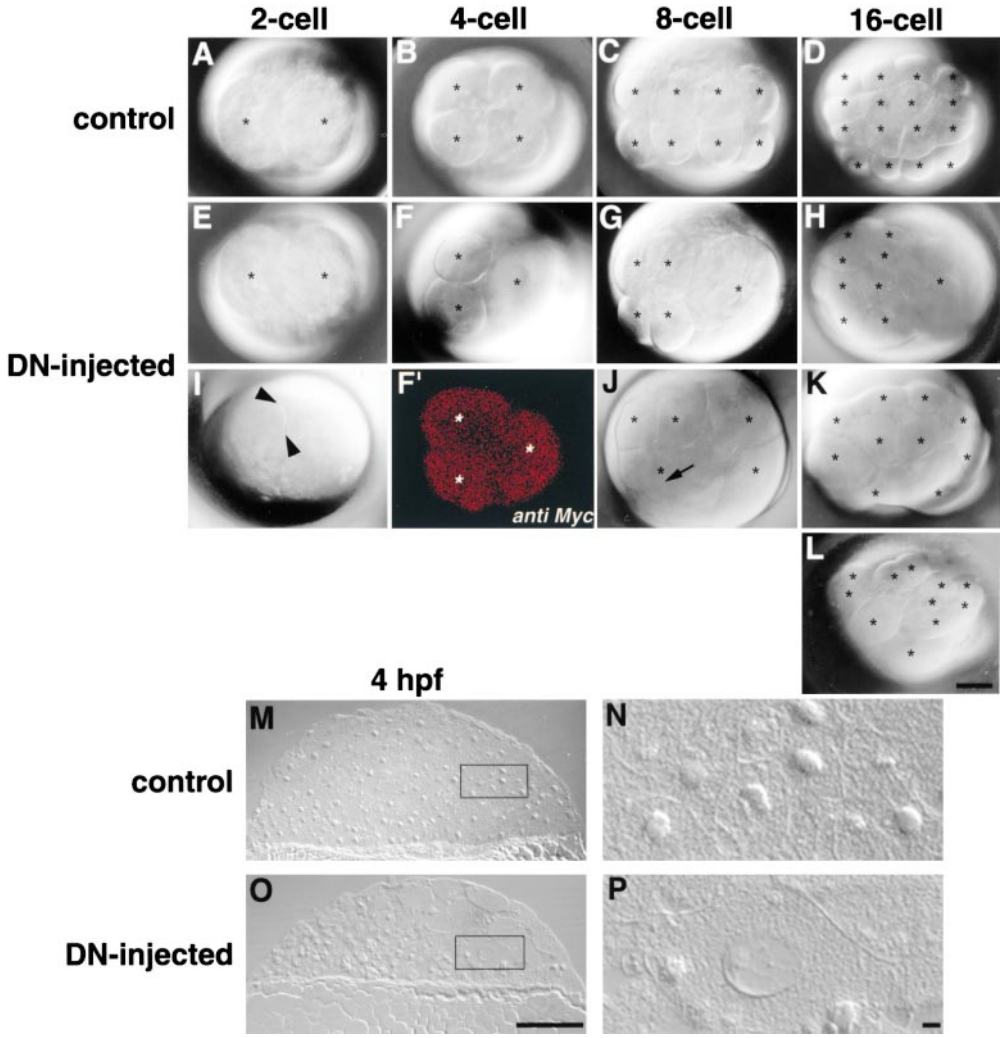

Figure 3 (continues on facing page).

DN-p38 phenotype when expressed in excess (Table I). The misexpression of WT-p38a RNA did not affect blastomere cleavage. Taken together, these results indicate that the cleavage defect phenotype was due to the suppression of p38 activity.

Expression of DN-MKK3 caused cleavage disruption similar to that observed in the DN-p38a–expressing embryos (Table I, for similar morphology see Fig. 3, E–L, DN-injected), and the cleavage defect was suppressed by excess amounts of WT-MKK3. In addition, injection of CA-MKK3 (125-250 pg RNA) at 10 mpf caused mitotic arrest by the four-cell stage. These results imply a role for the MKK3-p38 pathway in the regulation of blastomere cleavage, suggesting that proper activation of p38 on one side of the blastodisc is required for normal cleavage.

Impaired Cleavage Patterns Are Unrelated to the Orientation of the First Cleavage Plane

The cleavage defects in the DN-38a RNA–injected embryos were assigned to one of three categories (Fig. 3 Q, scheme). In the first category, blastomeres with incomplete cleavage were preferentially located on one side of the first cleavage plane (Fig. 3 Q, second column, 37.4% of total examined, $n = 322$; compare with first column, nor-

Table I. Percentages of Cleavage Disruption Observed after Injection of Synthetic mRNAs

RNA injected*	Percent disrupted cleavage‡	Percent nornal cleavage	Percent dead§	Total number tested
DNp38 (125)	82	18	0	300
DNp38/WTp38 (125/125)	73	27	0	222
DNp38/WTp38 (125/250)	60	39	1	123
DNp38/WTp38 (125/500)	0	69	31	198
WTp38 (250)	0	100	0	114
DNp38/WTJNK (125/500)	80	0	20	120
DNMKK3 (250)	61	39	0	210
DNMKK3/WTMKK3 (125/500)	0	70	30	118

*Synthetic RNAs encoding zebrafish WTMKK3, DNMKK3, WTJNK, WTp38a, or DNp38a were injected within 15 mpf. The relative amounts of the injected RNAs (in picograms) are given in parentheses.
‡Disrupted cleavage was defined as incomplete cleavage furrow formation at the 16-cell stage.
§Dead embryos were defined as fertilized embryos that underwent normal cleavages but failed to develop beyond the 16-cell stage.

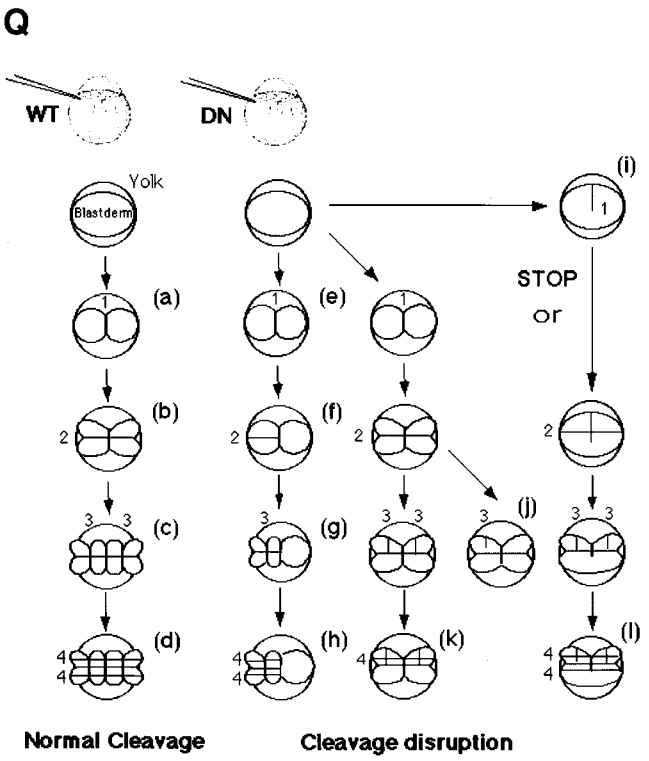

Figure 3. Impaired symmetric and synchronous cleavage by DN-p38. (A–D) Phenotypes after microinjection of the WT-p38a RNA (125 pg): 2-cell (A), 4-cell (B), 8-cell (C), and 16-cell stage (D). (E–L) Phenotypes after microinjection of the DN-p38a RNA (125–250 pg); DN-p38a RNA-injected embryos corresponding to the 2-cell (E and I), 4-cell (F), 8-cell (G and J), and 16-cell (H, K, and L) stage. (F–H) Incomplete cleavages were preferentially located on one side (right) of the first cleavage plane. (I, K, and L) Blastomeres with incomplete cleavages were preferentially located on one side (bottom portion) of the second cleavage plane. (I) Shortened cleavage furrow formation (arrowheads). Incomplete cleavages (arrows, the end of the cleavage furrow ingression) were observed in the intermediate region between the first and second cleavage planes (J). Localization of Myc-tagged DN-p38a (F′; see text). (M) Cross-sections of control embryos at the sphere stage (4 hpf). (N) Magnification of area outlined in M. (O) Cross-sections of the DN-p38a RNA-injected embryos at 4 hpf. (P) Magnification of outlined area in O. (Q) Schematic representation of cleavage formation. Each number denotes the order and sites of the cleavage furrow formation, and the letters in parenthesis correspond to the phenotypes shown in A–P. Asterisks mark each blastomere. Bars, 100 μm.

mal cleavage). In the second category, blastomeres with incomplete cleavage were preferentially located on one side of the future second cleavage plane (40.3% of the total examined; Fig. 3 Q, third and fifth columns). In the third category, blastomeres with impaired cleavage were observed in the intermediate region between the first and the second cleavage planes (22.3% of the total examined; Fig. 3 Q, fourth column). The incidence of these categories was examined in eight independent assays, indicating that the impaired cleavage patterns were unrelated to the orientation of the first cleavage plane ($n = 322$, d.f. $= 1$, $\chi^2 = 41.789$, $P < 0.001$). To further confirm this result, DN-p38a RNA was injected into the yolk cells at the zygote

Table II. Effects of SB203580 on Zebrafish Cleavage

Concentration of SB203580	*n*	Percent disrupted cleavage	Percent normal cleavage	Percent dead
μM				
10	120	40	60	0
100	138	100	0	0

Fertized embryos were incubated in SB203580 solution, prepared with the indicated concentrations, in E3 medium from the quiescent stage (10–15 mpf) and observed under a microscope at the 20-mpf and at the 16-cell stage to check the cleavage disruption. Embryos were counted at the 16-cell stage. Incubation in DMSO alone (up to 0.5%) did not affect cleavage of normal development.

stage (10 mpf), followed by the injection at the two-cell stage of a cell-tracing dye mixture, rhodamine/biotin-dextran (2,000 kD), into one blastomere of two-cell stage embryos (Fig. 4 A). By this procedure, DNp38 RNA was distributed uniformly in all the blastomeres, but only one blastomere and its daughters were labeled with the dye (Fig. 4 B). At the 1,000-cell stage, the labeled blastomeres were located on one side of the blastodisc (Fig. 4, C and D, cross-section) since cell mixing does not occur up to this stage (Abdelilah et al., 1994; Helde et al., 1994). The blastomeres with large amounts of cytoplasm and enlarged nuclei (Fig. 4, E–G, EN) were located on both the labeled side (Fig. 4 E, red) and the unlabeled side (Fig. 4, F and G), demonstrating that the polarity for the cleavage defect caused by the suppression of p38 did not correlate with the orientation of the first cleavage plane. Thus, there was no correlation between p38 activation and the site of the first cleavage formation.

Cleavage Disruption by DN-p38 Is Cell Autonomous

To reveal a cell-autonomous role for DN-p38 in the inhibition of blastomere cleavage, DN-p38a RNA was coinjected with the tracer dye rhodamine/biotin-dextran (2,000 kD) into one blastomere of the two-cell stage embryos (Fig. 5 A). In this case, 60.9% of the injected-embryos ($n = 64$) displayed the inhibition of symmetric cleavage, and the area displaying the cleavage defect always coincided with the labeled side at the 1,000-cell stage (Fig. 5 B, EN and red). In the DN-p38a–expressing embryos, cytokinesis was only perturbed (Fig. 6 E, red, phalloidin staining) while DNA synthesis normally underwent as BrdU was incorporated into DNA in the blastomere on DN-affected side (Fig. 6 D, green). This is consistent with the morphological observation at a later stage of DN-p38a–expressing embryos that contained abnormally enlarged nuclei (Fig. 3, O and P). These results allow us to draw two conclusions. First, DN-p38a disrupted cell cleavage only where it was functionally expressed, and its expression was sufficient to prevent p38 activation. Second, an inhibition of asymmetric p38 activation only impaired cytokinesis and, thus, disrupted symmetric cleavage patterns.

Site of the Cleavage Disruption by DN-p38a Correlates with the Future Dorsal Side

We next sought to address the possibility that the early asymmetry of the p38 activation might be linked to the polarity of the body axes, i.e., the dorso-ventral or right-left axes (Driever, 1995). In zebrafish, the initial cleavage

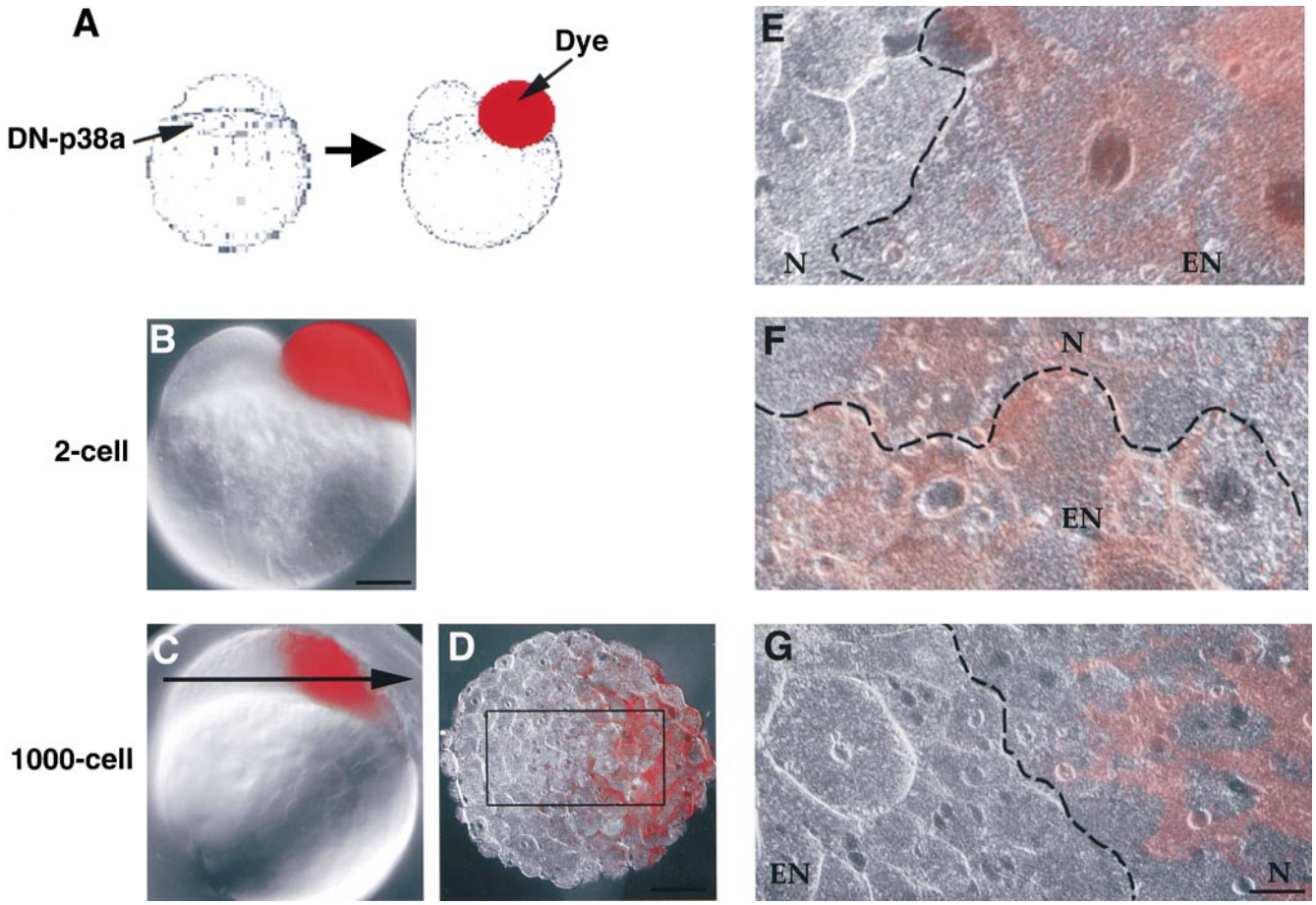

Figure 4. Cell lineage tracing. (A) DN-p38a RNA (125–250 pg) was injected into the yolk cell at 10 mpf, followed by the injection of a cell-tracing dye into one of the blastomeres at the two-cell stage. (B) Tracing dye (rhodamine/biotin-dextran, 2,000 kD) labeled one of the blastomeres of the two-cell stage embryos (red). (C) The labeled blastomere and its daughter cells (red) were located on one side of the blastodisc at the 1,000-cell stage. (D) Cross-section of DN-p38a RNA-injected embryo at the 1,000-cell stage (C, arrow, 100 μm from the animal pole surface). (E–G) Outlined area as in C. The blastomeres with cleavage defects were always located on the labeled side (red). (E–G) Marginal area (demarcated by dotted line) between normally divided (N) and enlarged blastomeres (EN). The blastomeres containing a large amount of cytoplasm and enlarged nucleus were strictly located on either the labeled (E) or the unlabeled side (G), or the labeled side included both enlarged and normal blastomeres (F). The red area in D–G is a superimposition of the tracing dye staining. Bars: (B and C) 110 μm; (D) 80 μm; (E–G) 4 μm.

plane does not correlate with the dorso-ventral axis or with the activation of p38 (Figs. 3 and 4; Abdelilah et al., 1994; Helde et al., 1994). We examined the expression of *dharma/bozozok* (Yamanaka et al., 1998), one of the earliest dorsal markers, in the DN-p38a–injected embryos. In control embryos, *dharma* transcripts were detected in a small group of the dorsal blastomeres at the mid-blastula stage (~3.3 hpf), and then in the dorsal yolk syncytial layer (YSL) from the late blastula to the early gastrula periods (Yamanaka et al., 1998; Fig. 7 A, arrowhead, dorsal side). In the DN-p38a–injected embryos, *dharma* transcripts were observed in both the blastoderm (Fig. 7 B, arrowhead) and the YSL (arrow) at the sphere stage. They were restricted to a few enlarged blastomeres (100%, n = 106) exclusively on one side of the blastoderm within the DN-affected area and also in the dorsal YSL. Thus, the blastomeres affected by the DN-p38 always coincided with the future dorsal side of the embryos. This result was also confirmed by examining thin sections of the embryos (Fig. 7 D; 100%, n = 30). The region of *dharma* expression appeared to have expanded in the DN-p38a–injected embryos because of their large cell mass and nuclei. These data provide a correlation between the site of the suppression of p38 activation and the future dorsal side of the embryos.

Effects of UV Irradiation and Yolk Removal on Asymmetric p38 Activation

We next addressed the question of whether or not p38 activation is controlled by the same machinery that regulates the formation of the dorso-ventral axis (see Introduction). For this investigation, we irradiated the embryos with UV light or removed the vegetal yolk mass. UV irradiation prevents the transport of the putative dorsal determinants to the dorsal side, and depletion of the yolk mass removes them from the embryo. We examined the effects of these procedures on the asymmetric activation of p38. When the

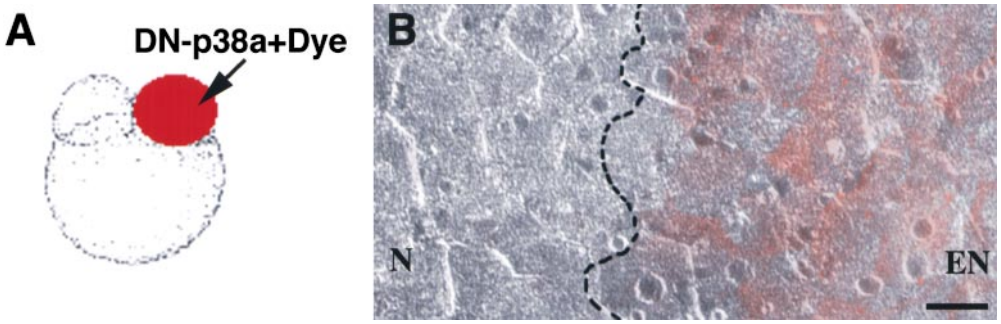

Figure 5. Cleavage disruption by DN-p38 is cell autonomous. (A) Cell-tracing dye (rhodamine/biotin-dextran, 2,000 kD) was injected together with DN-p38RNA (125–250 pg) into one of the blastomeres of two-cell embryos. (B) Cross-section of DN/dye-coinjected embryo (A) at 100 μm from the animal pole surface at the 1,000-cell stage. The marginal area, which is the same as that outlined in Fig. 4 D, is shown. Normally divided (N) and enlarged blastomeres (EN) are demarcated by a dotted line. Bar, 4 μm.

zygote stage (10 mpf) embryos were irradiated with 312 nm of UV light for 10 min, they displayed various developmental defects (n = 58; 51.7% gastrulation defects, 15.5% anterior truncation, and 8.7% epiboly arrest) as previously reported (Jesuthasan and Stahle, 1997). UV treatment at this stage eliminated the asymmetric activation of p38 (Fig. 8 B), although the p38 protein was uniformly expressed (Fig. 8 A). In contrast, when the embryos were treated with UV light at 25 mpf (two-cell stage), about half of the embryos developed normally (n = 62, 54.3%), and the rest displayed only epiboly defects. In good correlation with the observed phenotypes, the asymmetric or otherwise a ubiquitous activation of p38 was restored in the embryos treated later than 25 mpf (Fig. 8, compare D with C, p38 protein), indicating that signaling components that link a stress-mediated signal such as UV irradiation and

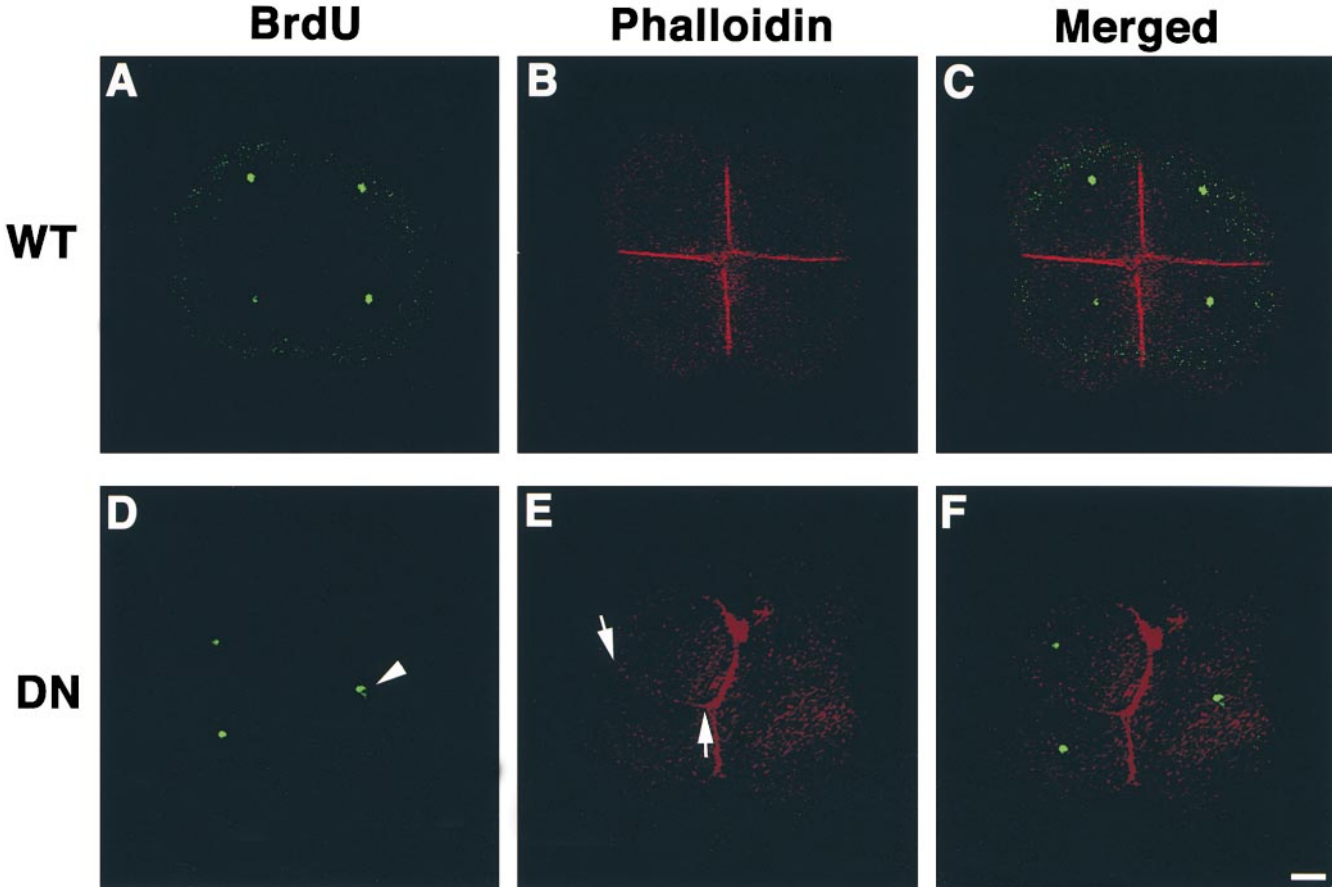

Figure 6. Inhibition of p38 activation perturbs cytokinesis on one side of the blastomere. (A) BrdU staining of WT-p38aRNA–injected (125 pg) embryo. (B) Phalloidin staining of A. (C) Merged view of A and B. (D) BrdU staining of DN-p38a RNA–injected(125 pg) embryo. (E) Phalloidin staining of D. (F) Merged view of D and E. Cleavage furrow only formed on one side of the DN-p38a RNA–injected embryos (arrows) because of an incomplete mitotic segregation or cytokinesis on another side of the blastomere (arrowhead). Bar, 100 μm.

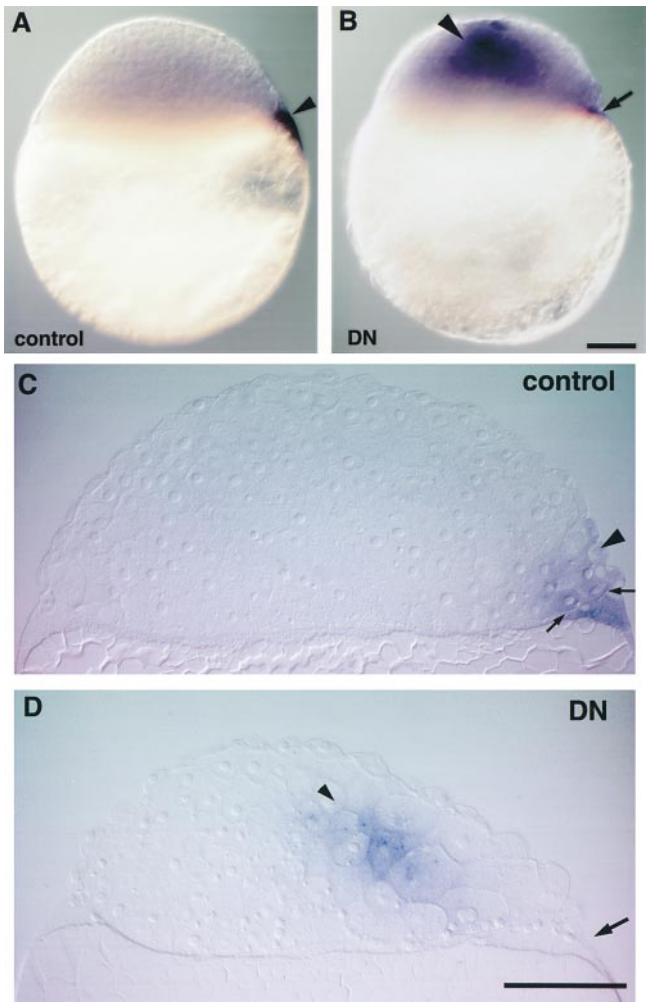

Figure 7. Expression of *dharma/bozozok* in DN-p38a–expressing embryos. Whole-mount in situ hybridization with *dharma* RNA probe of WT-p38a or DN-p38a RNA–injected embryos (125–250 pg) is shown. In control embryos, *dharma* transcripts were detected in a small group of the blastomeres and the YSL on the future dorsal side at the sphere stage (A, arrowhead). In DN-p38a RNA–injected embryos, *dharma* transcripts were detected both in the enlarged cells inside the blastoderm (B, arrowhead) and the dorsal YSL (arrow) at 4 hpf. (C) Sagittal section of A: (arrowhead) *dharma*-expressing blastomeres; and (arrows) margin of the YSL. (D) Sagittal section of B: (arrowhead) *dharma* expression inside the blastoderm; and (arrow) the dorsal YSL. Bars, 100 μm.

MKK3-p38 pathway might be missing before 25 mpf. These data strongly suggest that the vegetal microtubule array formed at ~10 mpf could be involved in the transport of not only the dorsal determinants, but also an activator for the p38 pathway, or else that the vegetal microtubule array might, by itself, be involved in the activation of p38.

Next, we examined whether p38 activation depends on factors located in the vegetal yolk region. When the vegetal yolk mass was removed as early as the one-cell stage, the embryos displayed a completely ventralized phenotype with no dorsal and anterior structures (data not shown) as previously reported (Mizuno et al., 1999b). In these yolk-depleted embryos, no expression of *dharma* was detected at any developmental stage (30/30; Fig. 9 A, compare with controls on which no operation was performed) and the p38 asymmetric activation at the early cleavage stages was completely missing (20/20; Fig. 9 C), although the p38 protein was evenly distributed (Fig. 9 B). These results suggest that the asymmetrical activation of p38 is dependent on unknown factors (Fig. 10, "X") located in the vegetal yolk hemisphere, just as the dorsalizing signals are dependent on the dorsal determinants located there.

Discussion

p38 is a member of the MAP kinase family, which is conserved from yeast to vertebrates. Although the functions of p38 in stress responses are relatively well documented, its role in development has not been fully elucidated. Here, we show that p38 in zebrafish is asymmetrically activated during the cleavage period, and may play a role in cleavage control on the prospective dorsal side. First, using an antibody specific to the dually phosphorylated activated form of p38, we showed that activated p38 protein was localized to only one side of the embryo (Fig. 2). The location of activated p38 did not correlate with the orientation of the initial cleavage plane (Fig. 4). Second, overexpression of DN-p38a asymmetrically inhibited mitotic segregation (or cytokinesis) of the blastomeres only on one side in a cell-autonomous manner (Fig. 5), probably by sequestering upstream activators for endogenous p38a (Figs. 8 and 9). The DN-p38a–affected blastomeres had large amounts of cytoplasm with enlarged nuclei (Fig. 3), further indicating that p38 activity is required for cytokinesis but not for DNA replication during the cleavage period (Fig. 6). The effect of DN-p38a was specific since its effect was rescued by excess amounts of WT-p38a but not JNK. Moreover, inhibition of p38 by the p38-specific inhibitory compound SB203580 and also by DN-MKK3 exhibited a similar effect on blastomere cleavage as did DN-p38a (Table II). Thus, DN-p38a may inhibit p38 where it is initially activated.

Regulation of Asymmetric Activation of p38 on the Prospective Dorsal Side

Transcripts of the earliest dorsal marker *dharma* were always detected in the enlarged blastomeres induced by DN-p38a. Furthermore, disruption of microtubules by UV irradiation at 10 mpf or depletion of the vegetal yolk material, which are known to abolish the dorsalizing signals, inhibited the asymmetric activation of p38 during the early cleavage period. Nonetheless, the asymmetry in both p38 activation and in the cleavage defects elicited by DN-p38a did not correlate with the initial cleavage plane. This result is consistent with previous reports indicating that the orientation of the dorso-ventral axis is apparently random with respect to the first or second cleavage plane in zebrafish (Abdelilah et al., 1994; Helde et al., 1994). Taken together, our results indicate a striking link between the machinery that induces asymmetric activation of p38 and the signals that determine the future dorsal side. This raises the possibility that a putative p38 activator "X," which is present at the vegetal pole, is transported to-

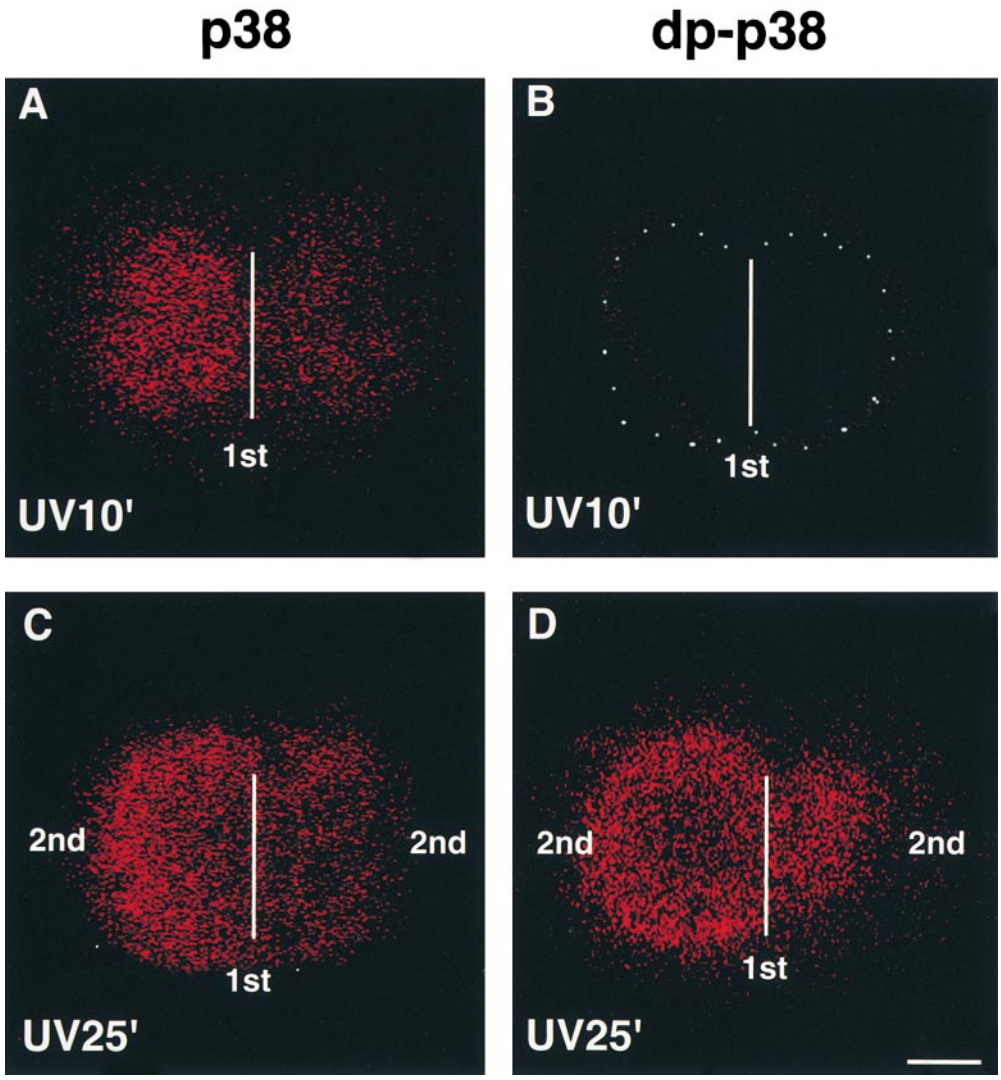

Figure 8. Effects of UV irradiation on asymmetric p38 activation before the first cleavage formation. Immunostaining of the embryos by either anti-p38 antibody (A and C) or anti–dp-p38 antibody (B and D) after UV irradiation (312 nm) for 10 min from 10 mpf (A and B) or from 25 mpf (C and D) was viewed using a confocal microscope. Asymmetric p38 activation (see Fig. 1, B and C) was totally abolished by UV irradiation at 10 mpf (B, dotted line, outline of the blastodisc). (D) Activation of p38 after UV irradiation at 25 mpf. White lines indicate the site of the first cleavage furrow formation at the two-cell stage. Images were taken as described in the legend for Fig. 1. Bar, 100 μm.

gether with or without dorsal determinants via the microtubule array (Fig. 10).

Dorsal determinants, which are initially located at the vegetal pole of the yolk, are thought to be transported to the blastodisc as early as the 16–32-cell stage in zebrafish since perturbation of microtubule formation before, but not after, this stage ventralizes the embryos (Driever, 1995; Jesuthasan and Stahle, 1997). In our study, the asymmetric p38 activation was first detected by the two-cell stage. Asymmetric activation of the dorsalizing signals and of p38 were dependent on the putative vegetal yolk factors, dorsal determinants, and an unknown p38 activator, respectively, and also on the microtubule array formation in the yolk. A putative p38 activator appeared to be transported to the putative dorsal side via the microtubule arrays, preceding the dorsal determinants, and suggesting that the putative p38 activator may be distinct from the dorsal determinants. However, it is also possible that small amounts of the dorsal determinants might be transported before the two-cell stage, and could be sufficient for the activation of the p38 pathway, but not for activating the dorsalizing signals.

One candidate for the p38 activator is a Dishevelled homologue (Dvl). Recently, it has been reported that Dishevelled proteins are translocated from the vegetal pole to the dorsal side of embryos through the microtubule array, after cortical rotation, in *Xenopus* (Moon and Kimelman, 1998; Miller et al., 1999). *Drosophila* genetics and biochemical analyses show that Dishevelled and Dvls mediate a signal to JNK, which shares an upstream activator with p38 (Boutros et al., 1998; Paricio et al., 1999). In NIH3T3 cells, mouse Dvl-1 activates *Xenopus* p38 (Moriguchi et al., 1999). We also found that overexpression of zebrafish Dvl3 in 293T cells elicited the dual phosphorylation in the TGY motif of p38 and activated ATF2-dependent transcription through p38 (R. Fujii and T. Hirano, unpublished data). Further analyses will be required to clarify the role of Dvl in asymmetric p38 activation. Identification of the upstream components of the MKK3-p38 signaling pathway will provide clues that will help us understand the mechanisms that control asymmetry during the cleavage period. Recent studies have shown that intense free calcium pulses are observed at the forming cleavage furrows of zebrafish embryos from the 2-cell

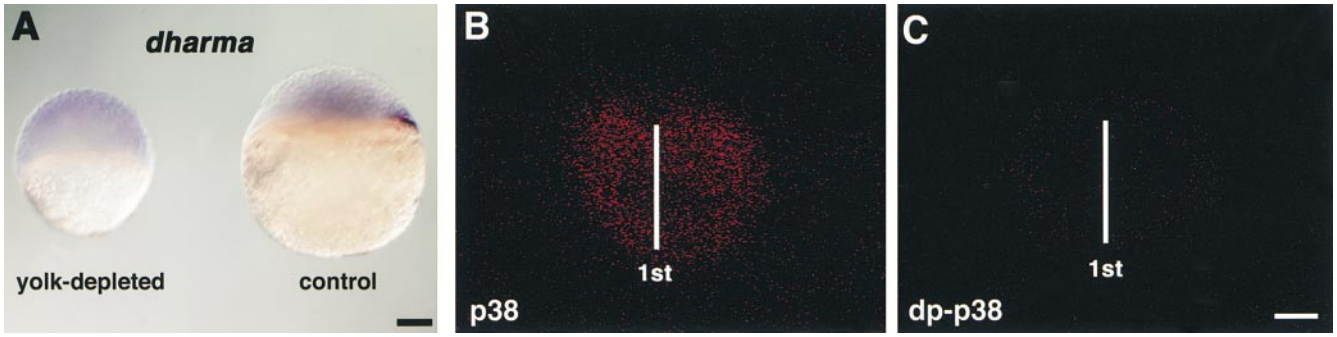

Figure 9. Effects of yolk removal on p38 activation and *dharma/bozozok* expression. (A) Whole-mount in situ hybridization by *dharma* RNA probe. Removal of the vegetal yolk hemisphere abolished the expression of *dharma* (A, left indicated as yolk-depleted; 100%, n = 30) at the sphere stage. *dharma* transcripts were detected in the dorsal YSL of the control on which no operation was performed (right). (B) Immunostaining of the yolk-depleted embryo at the two-cell stage by anti-p38 antibody to show the distribution of p38, and p38 activation was probed using the anti–dp-p38 antibody (n = 20) (C). Images were taken as described in the legend for Fig. 1. Bars, 100 μm.

through the 16-cell stage (Creton et al., 1998). It would be interesting to investigate if there is a link between the calcium signal and the p38 activation.

Although there is strong correlation between p38 activation and the formation of the dorsal side, overexpression of DN-p38a did not inhibit the expression of *dharma* or ectopically induced it. Thus, the MKK3-p38 pathway may not be directly involved in dorso-ventral determination.

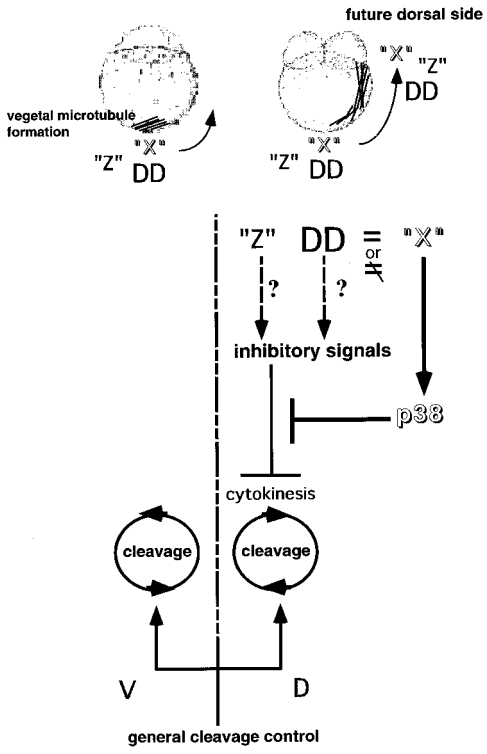

Figure 10. The asymmetric p38 activation is required for symmetric and synchronous cleavage in zebrafish. "X," unknown factor(s) transported from the vegetal pole through the vegetal microtubule array. DD, dorsal determinants; and "Z," putative signal(s) transported from the vegetal pole through the vegetal microtubule array that compete with p38. V, ventral side; D, dorsal side.

Control of Cleavages by Asymmetric p38 Activation

p38 was activated on the future dorsal side of the blastodisc, and its activity was required for cytokinesis on the same side (Fig. 6). Why are the symmetric and synchronous cleavages controlled by the asymmetrically activated p38? Intriguingly, a time frame of the asymmetric p38 activation correlates with stages when all the blastomeres are continuous with the yolk. The most likely possibility is that the formation of cortical microtubule arrays in the future dorsal side of the yolk results in the asymmetrical transportation or activation of unknown signals that inhibit cytokinesis, which is accompanied by a correct mitotic spindle formation (Fig. 10). Whether or not the putative activator for p38 (Fig. 10, "X") is a dorsal determinant (which is also transported to the future dorsal side via the microtubule arrays), it may activate p38 and, in turn, suppress the inhibitory signals to maintain the normal cleavage pattern. Consistent with this scenario, UV irradiation at 10 mpf or yolk removal resulted in the same normal blastomere cleavage. One interpretation of this result is that these treatments, which also inhibit the transportation of dorsal determinants, attenuated not only the activity of "X," but also those of the putative inhibitory signals for the cleavage pattern.

A present open question is what induces such inhibitory signals? One possibility is that the dorsal determinants intrinsically activate the inhibitory signals and thereby they must activate p38 at the same time to cancel the inhibitory signals, thus, permitting proper cleavages to take place. This speculation does not conflict with the fact that there is no report that inhibition of the Wnt pathway, which is strongly implicated in dorsalizing signals (Sokol, 1999), elicits cleavage defects. Alternatively, other unknown signals activated by the putative yolk factor (Fig. 10, "Z") may compete with the p38 signal. In any case, p38 may play a role in canceling the coexisting inhibitory signals or directly regulate cytokinesis, probably by acting on spindle microtubules, which is inhibited by the yolk-derived signals. What is activated by p38 should be identified to clarify these issues.

Because asymmetric cell division is a common pattern for the initial cleavage in invertebrates, it is tempting to speculate that asymmetric cell division is the default for

the initial cleavage. In vertebrates, evolutionary force might have made symmetric cleavage necessary for proper development, and thereby asymmetric mechanisms have evolved. Supporting our hypothesis, the *Drosophila* MKK3-p38 pathway has been reported to be essential for the correct asymmetric development of oocytes (Suzanne et al., 1999), such as the establishment of both the anterior-posterior and the dorso-ventral axes. In this paper, we provide a model that the asymmetric p38 activation could be intrinsic to the control of symmetric and synchronous cleavage in zebrafish. Our novel implication of the p38 pathway in both blastomere cleavage and the initial dorsal patterning sheds new light on the understanding of when and how a vertebrate embryo acquires polarity through cleavage.

We thank Rie Fukunaga and Yukiko Kuga for excellent technical support, and Drs. Motoyuki Itoh and Hisashi Hashimoto for valuable suggestions. We give special thanks to Dr. Yojiro Yamanaka for sharing data from his previous work on *dharma*.

This work was supported by grants and a Grant-in-Aid for Center of Excellence (COE) Research from the Ministry of Education, Science, Sports and Culture in Japan.

Submitted: 2 March 2000
Revised: 1 August 2000
Accepted: 1 August 2000

References

Abdelilah, S., L. Solnica-Krezel, D.Y. Stainier, and W. Driever. 1994. Implications for dorsoventral axis determination from the zebrafish mutation janus. *Nature*. 370:468–471.

Boutros, M., N. Paricio, D.I. Strutt, and M. Mlodzik. 1998. Dishevelled activates JNK and discriminates between JNK pathways in planar polarity and wingless signaling. *Cell*. 94:109–118.

Creton, R., J.E. Speksnijder, and L.F. Jaffe. 1998. Patterns of free calcium in zebrafish embryos. *J. Cell. Sci.* 111:1613–1622.

Davis, R.J. 1999. Signal transduction by the c-Jun N-terminal kinase. *Biochem. Soc. Symp*. 64:1–12.

Derijard, B., J. Raingeaud, T. Barrett, I.H. Wu, J. Han, R.J. Ulevitch, and R.J. Davis. 1995. Independent human MAP-kinase signal transduction pathways defined by MEK and MKK isoforms [published erratum appears in *Science*. 1995. 269:17]. *Science*. 267:682–685.

Driever, W. 1995. Axis formation in zebrafish. *Curr. Opin. Genet. Dev*. 5:610–618.

Enslen, H., J. Raingeaud, and R.J. Davis. 1998. Selective activation of p38 mitogen-activated protein (MAP) kinase isoforms by the MAP kinase kinases MKK3 and MKK6. *J. Biol. Chem*. 273:1741–1748.

Garrington, T.P., and G.L. Johnson. 1999. Organization and regulation of mitogen-activated protein kinase signaling pathways. *Curr. Opin. Cell Biol*. 11: 211–218.

Gupta, S., D. Campbell, B. Derijard, and R.J. Davis. 1995. Transcription factor ATF2 regulation by the JNK signal transduction pathway. *Science*. 267:389–393.

Han, J., J.D. Lee, L. Bibbs, and R.J. Ulevitch. 1994. A MAP kinase targeted by endotoxin and hyperosmolarity in mammalian cells. *Science*. 265:808–811.

Helde, K.A., E.T. Wilson, C.J. Cretekos, and D.J. Grunwald. 1994. Contribution of early cells to the fate map of the zebrafish gastrula. *Science*. 265:517–520.

Ho, S.N., H.D. Hunt, R.M. Horton, J.K. Pullen, and L.R. Pease. 1989. Site-directed mutagenesis by overlap extension using the polymerase chain reaction. *Gene*. 77:51–59.

Jesuthasan, S., and U. Stahle. 1997. Dynamic microtubules and specification of the zebrafish embryonic axis. *Curr. Biol*. 7:31–42.

Kane, D.A. 1999. Cell cycles and development in the embryonic zebrafish. *Methods Cell Biol*. 59:11–26.

Kodjabachian, L., I.B. Dawid, and R. Toyama. 1999. Gastrulation in zebrafish: what mutants teach us. *Dev. Biol*. 213:231–245.

Larabell, C.A., M. Torres, B.A. Rowning, C. Yost, J.R. Miller, M. Wu, D. Kimelman, and R.T. Moon. 1997. Establishment of the dorso-ventral axis in *Xenopus* embryos is presaged by early asymmetries in β-catenin that are modulated by the Wnt signaling pathway. *J. Cell Biol*. 136:1123–1136.

Lee, J.C., J.T. Laydon, P.C. McDonnell, T.F. Gallagher, S. Kumar, D. Green, D. McNulty, M.J. Blumenthal, J.R. Heys, S.W. Landvatter, et al. 1994. A protein kinase involved in the regulation of inflammatory cytokine biosynthesis. *Nature*. 372:739–746.

Mansour, S.J., W.T. Matten, A.S. Hermann, J.M. Candia, S. Rong, K. Fukasawa, G.F. Vande Woude, and N.G. Ahn. 1994. Transformation of mammalian cells by constitutively active MAP kinase kinase. *Science*. 265: 966–970.

Miller, J.R., B.A. Rowning, C.A. Larabell, J.A. Yang-Snyder, R.L. Bates, and R.T. Moon. 1999. Establishment of the dorsal-ventral axis in *Xenopus* embryos coincides with the dorsal enrichment of dishevelled that is dependent on cortical rotation. *J. Cell Biol*. 146:427–438.

Mizuno, T., M. Shinya, and H. Takeda. 1999a. Cell and tissue transplantation in zebrafish embryos. *Methods Mol. Biol*. 127:15–28.

Mizuno, T., E. Yamaha, A. Kuroiwa, and H. Takeda. 1999b. Removal of vegetal yolk causes dorsal deficiencies and impairs dorsal-inducing ability of the yolk cell in zebrafish. *Mech. Dev*. 81:51–63.

Moon, R.T., and D. Kimelman. 1998. From cortical rotation to organizer gene expression: toward a molecular explanation of axis specification in *Xenopus*. *Bioessays*. 20:536–545.

Moriguchi, T., K. Kawachi, S. Kamakura, N. Masuyama, H. Yamanaka, K. Matsumoto, A. Kikuchi, and E. Nishida. 1999. Distinct domains of mouse dishevelled are responsible for the c-Jun N-terminal kinase/stress-activated protein kinase activation and the axis formation in vertebrates. *J. Biol. Chem*. 274:30957–30962.

Paricio, N., F. Feiguin, M. Boutros, S. Eaton, and M. Mlodzik. 1999. The *Drosophila* STE20-like kinase misshapen is required downstream of the Frizzled receptor in planar polarity signaling. *EMBO (Eur. Mol. Biol. Organ.) J*. 18: 4669–4678.

Raingeaud, J., S. Gupta, J.S. Rogers, M. Dickens, J. Han, R.J. Ulevitch, and R.J. Davis. 1995. Pro-inflammatory cytokines and environmental stress cause p38 mitogen-activated protein kinase activation by dual phosphorylation on tyrosine and threonine. *J. Biol. Chem*. 270:7420–7426.

Raingeaud, J., A.J. Whitmarsh, T. Barrett, B. Derijard, and R.J. Davis. 1996. MKK3- and MKK6-regulated gene expression is mediated by the p38 mitogen-activated protein kinase signal transduction pathway. *Mol. Cell. Biol*. 16: 1247–1255.

Rupp, R.A., L. Snider, and H. Weintraub. 1994. *Xenopus* embryos regulate the nuclear localization of XMyoD. *Genes Dev*. 8:1311–1323.

Sokol, S.Y. 1999. Wnt signaling and dorso-ventral axis specification in vertebrates. *Curr. Opin. Genet. Dev*. 9:405–410.

Suzanne, M., K. Irie, B. Glise, F. Agnes, E. Mori, K. Matsumoto, and S. Noselli. 1999. The *Drosophila* p38 MAPK pathway is required during oogenesis for egg asymmetric development. *Genes Dev*. 13:1464–1474.

Westerfield, M. 1995. The Zebrafish Book: A Guide for the Laboratory Use of Zebrafish (*Danio rerio*). Institute of Neuroscience, University of Oregon, Eugene, OR.

Yamanaka, Y., T. Mizuno, Y. Sasai, M. Kishi, H. Takeda, C.H. Kim, M. Hibi, and T. Hirano. 1998. A novel homeobox gene, *dharma*, can induce the organizer in a non-cell-autonomous manner. *Genes Dev*. 12:2345–2353.